The Potential of Multi temporal SAR Time Series Analysis for the Monitoring of the Geobattery Project

Maria Carmelia RAMLIE[1,*], **Paula OLEA-ENCINA**[1], **Christophe MAGNARD**[2], **Tazio STROZZI**[2], **Oriol MONSERRAT**[1], **Michele CROSETTO**[1], and **Cristopher McDERMOTT**[3]

[1] *CTTC, Castelldefels, Spain, (mramlie, omonserrat, polea, mcrosetto@cttc.cat)*

[2] *GAMMA Remote Sensing, Gümligen (BE), Switzerland, (magnard, strozzi@gamma-rs.ch)*

[3] *University of Edinburgh, Edinburgh, Scotland, (christopher.mcdermott@ed.ac.uk)*

[*] *corresponding author*

Abstract

Geobattery is a geothermal project with the concept of transporting recyclable heat to nearby population via elevated permeability pathways in the subsurface and offering a platform for managing shallow geothermal resources. Midlothian on the Southeastern part of Scotland was chosen for this project due to the significant potential from the abandoned coal mine workings, particularly the Burghlee, Roslin, and Ramsay colliery mine workings. Time series analysis is proposed for a method for monitoring and analyzing the project as it offers the potential to detect millimetre scale deformation over large area while providing the flexibility and practicality of remote sensing technology. We aim to integrate PSI analyses from multiple satellite SAR sensors with different frequencies, acquisition time intervals and spatial results in order to gain maximum information. In this preparatory study, ALOS-2 PALSAR-2 L-band data are used, which generally works better over vegetated areas. The result of the processing indicates an uplift, possibly caused by the flooding of the mines since the pump stopped. The uplift may need to be considered with regard to the future of the project and its impact on the surrounding areas.

Keywords: geothermal, remote sensing, satellite SAR, PSI, deformation monitoring

Received: 10th December 2024. Revised: 24th February 2025. Accepted: 25th February 2025.

1 Introduction

Geothermal energy, the Earth's internal heat, is a vast yet underutilized renewable resource that provides stable, low-carbon baseload power. Despite its potential, challenges such as deep resource accessibility and uneven global distribution hinder its widespread adoption. Successful geothermal projects require accessible reservoirs, permeable rock formations, and sufficient fluids for heat transfer. However, extraction and injection processes can alter subsurface conditions, leading to potential ground deformation, which necessitates continuous monitoring to ensure operational safety.

One promising innovation is the Geobattery (Fraser-Harris et al., 2022) for Midlothian, Edinburgh. This concept envisions a circular heat network that redistributes recyclable heat, utilizes natural subsurface permeability, and enhances urban energy resilience. To ensure safe and efficient operation, precise monitoring is essential, particularly in tracking ground deformation caused by geothermal processes. Satellite SAR interferometry, particularly Persistent Scatterer Interferometry (PSI), offers a sophisticated tool for assessing these changes. Previous studies (Nam et al., 2021; Van Anh et al., 2020) have demonstrated PSI's effectiveness in monitoring surface deformation, making it a valuable technique for geothermal applications.

To optimize geothermal monitoring, we propose integrating multiple satellite sensors with varying properties, including Sentinel-1 (C-band), Cosmo-SkyMED (X-band), and ALOS-2 PALSAR-2 (L-band) in the future. This multi-sensor approach enhances deformation detection, particularly in urban and vegetated areas. In this preparatory study,

we focus on the potential and technical challenges of ALOS-2 PALSAR-2, aiming to refine its application for monitoring geothermal projects like the Geobattery. By incorporating advanced satellite technologies, this research supports the development of a sustainable, low-carbon, and resilient heating solution.

2 Study Area: Midlothian, Edinburgh, Scotland

In the United Kingdom, the potential of abandoned mines for geothermal renewable heat and thermal energy storage is increasingly recognized. This is particularly relevant in areas where a significant portion of housing and businesses are situated above legacy flooded coal mines, such as in Midlothian. Approximately one quarter of properties in the UK are located over coalfields (Banks et al., 2019, 2009; Gluyas et al., 2020; Mining Remediation Authority, 2024), presenting unique opportunities for geothermal energy exploitation. The United Kingdom have announced plans to prevent installation of fossil fuel-based heating system after 2025 and committing on developing heat pump installations and increase in investment towards developing mine water geothermal schemes.

Figure 1. The proposed potential area of Midlothian on the Southeastern part of Scotland (United Kingdom) by Edinburgh is indicated within the red circle.

Midlothian, located in southeastern Edinburgh, Scotland, has been selected for the Geobattery project due to its geological condition and potential for geothermal energy development. Historically known as a mining district, the area is dotted with abandoned mines that offer promising prospects for geothermal energy. Geologically, Midlothian is characterized by a basin of Carboniferous rocks surrounded by igneous formations and lower Paleozoic greywackes. The region features thick layers of glacial, post-glacial, and alluvial deposits over its lowlands. These geological formations have been shaped by various processes over millions of years.

The historical significance of Midlothian's geology extends beyond its natural resources. The fertile lowlands and proximity to coastal routes facilitated early human settlement and industrialization. This rich history is reflected in the area's cultural heritage and economic development over centuries. By understanding the geological and historical context of Midlothian, we can better appreciate its potential for innovative geothermal projects like the Geobattery. This project not only leverages the area's natural resources but also aims to contribute to sustainable development and energy resilience in the region.

3 Data and Processing

3.1 ALOS-2/PALSAR-2 PSI

The proposed technique to monitor deformation over the Midlothian test area is Persistent Scatterer Interferometry (PSI), an advanced DInSAR technique that focuses on exploiting a large stacks of SAR images. Several PSI techniques have been proposed in the last decade, including Persistent Scatterers (Ferretti et al., 2001), Small Baseline Subset (SBAS) (Berardino et al., 2002), Stable Point Network (SPN), and Interferometric Point Target Analysis (IPTA) (Werner et al., 2003).

We apply a multi-baseline time-series analysis to a stack of Stripmap images obtained from ALOS-2 PALSAR-2 over Edinburgh, Scotland, using the Gamma software (Werner et al., 2003). A total of 16 images were acquired between 2014 and 2024 at HH polarization (Table 1 and Figure 2).

Table 1. ALOS2/PALSAR2 Scenes

No.	ALOS2/PALSAR2
	Stripmap
	Date
1	10/12/2014
2	18/2/2015
3	8/6/2016
4	28/9/2016

5	15/2/2017
6	19/7/2017
7	31/1/2018
8	18/7/2018
9	29/8/2018
10	7/11/2018
11	22/5/2019
12	20/5/2020
13	19/5/2021
14	18/5/2022
15	5/4/2023
16	3/4/2024

3.2 Initial Processing

The initial processing workflow consisted of several key stages such as preparation of the reference image, Digital Terrain Model (DTM), geocoding of the reference image and co-registration of all the images to the reference image. From the diagram of Figure 2, the data from 18 July 2018 was chosen as the reference image and all the other images were co-registered to this image. The reference image was also used to generate a reference lookup table for future geocoding.

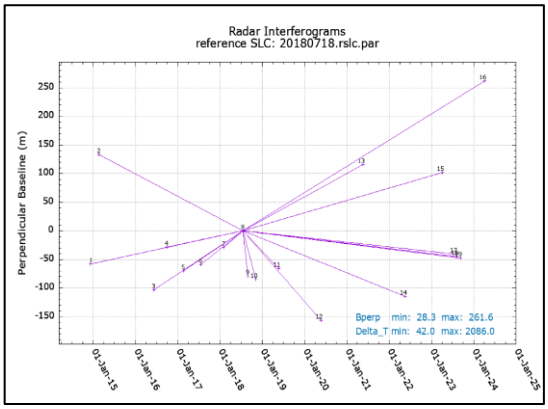

Figure 2. Diagram of the distribution of the perpendicular baselines of the Stripmap ALOS-2 PALSAR-2 data over Edinburgh as a function of the acquisition date. The acquisition of 18 July 2018 is selected as geometric reference.

3.3 Interferogram Generation

We implemented a multi-referencing strategy for time series PSI processing (Berardino et al., 2002). This approach involves pairing each scene with subsequent scenes using a maximum temporal baseline of three years (Figure 3).

The multi-referencing strategy offers several advantages such as enhanced redundancy, facilitating more robust phase unwrapping, improved coherence, mitigating unwrapping difficulties, and reduced deformation phase, simplifying the unwrapping process.

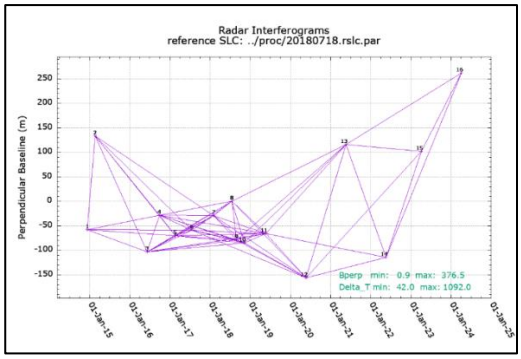

Figure 3. Diagram presenting the pairing of each scene with subsequent scenes using a temporal baseline of three years.

By employing this methodology, the aim is to increase the reliability and accuracy of our interferometric analysis in this challenging terrain.

3.4 Phase Unwrapping

The initial attempt at phase unwrapping revealed significant challenges, primarily due to low coherence and the presence of phase artifacts across the study area. In particular, severe phase ramps were found in interferograms generated from images acquired using different center frequencies. Low coherence and strong phase variations most likely linked to ionospheric perturbations were also detected in interferograms formed using one of the acquisitions. To overcome these challenges and improve the quality of the phase unwrapping process, we applied the following strategies.

3.4.1 Identification of frequency discrepancies

The first two images of the time-series, acquired on 10 December 2014 and 18 January 2015, were have a slightly higher center frequencies than the rest of the time-series. Without correction, interferograms formed using one of the two first images and one image from the rest of the time-series would result in phase noise. To overcome this, we synthetically shifted the center frequency of the two first images to the same value as that of the rest of the time-series stack and applied a common band. The shift of frequencies resulted in the recovery of some coherence for all the images that were paired with

the 2 first images, however severe phase ramps were observed in these interferograms (Figure 4).

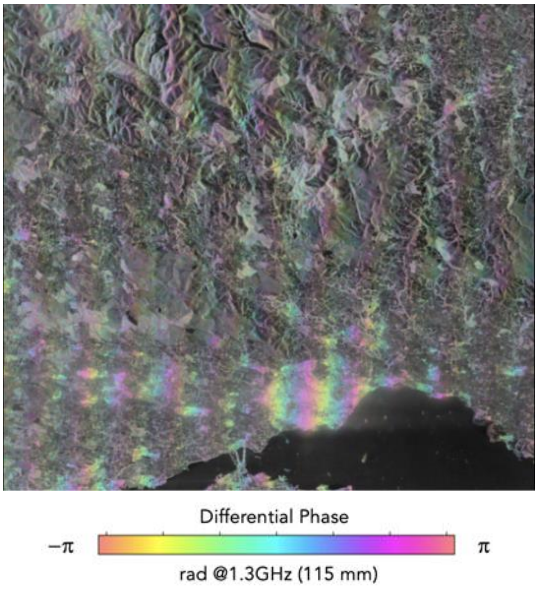

Figure 4. An interferogram of image pair 10 December 2014 and 6 August 2016 showing a phase ramp.

Linear phase ramps were estimated for all the interferograms from an initial phase unwrapping solution. They were then subtracted from the interferograms, resulting in a much "flatter" interferometric phase in particular for the interferometric pairs using the two first images (figure 5).

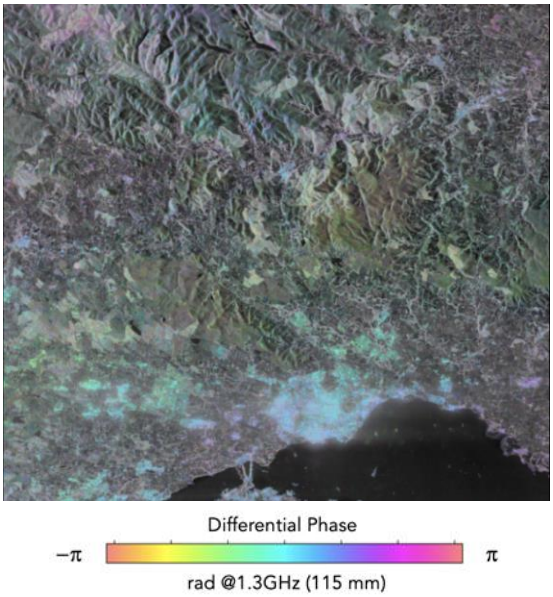

Figure 5. A frequency shifted image of 10 December 2014 paired with 6 August 2016 after linear phase ramp subtraction.

3.4.2 Ionospheric Path Delay

Anomalies in interferograms paired with the 5 April 2023 scene (see e.g. Figure 6) led to an investigation of ionospheric path delay. Ionosphere is an outer most layer of Earth's atmosphere containing relatively large number of electrically charged atoms and molecules. SAR satellites are located on an altitude of more than 500 km, i.e. above the ionosphere. In the case of low radar frequencies, such as L-band, spatial and temporal variation in the free electron concentration in the ionosphere will affect SAR interferograms with loss of coherence, image deformations, and phase distortions (Meyer and Nicoll, 2008; Wegmüller et al., 2024).

Ionospheric effect was speculated to be present on image dated 5 April 2024 that affects the phase unwrapping stage. To see if the low coherence area with large phase variations was indeed affected by ionospheric delay, an ionospheric check was employed. For that purpose, we determined the azimuth spectrum sub-band range and azimuth offsets of the 5 April 2024 image. Significant non-zero azimuth offsets are clearly visible (Figure 6) and indicate the presence of ionospheric effects.
In order to mitigate the effects of the ionospheric perturbations, we applied a co-registration refinement by estimating an offset field relative to the geometric reference and resampling the image accordingly. This resulted in a much-improved coherence in interferograms paired with that image.

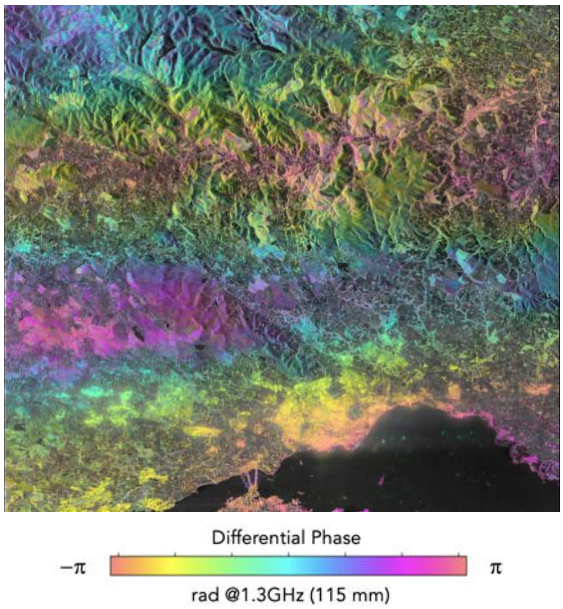

Figure 6. The interferogram of 5 April 2023 paired with 3 April 2024 after refined co-registration, showing the existence of ionospheric phase delay.

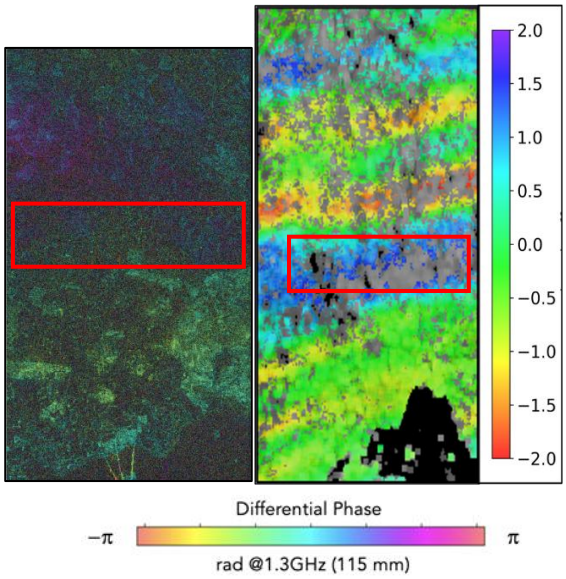

Figure 7. (Left) Interferogram between 5 April 2023 and 3 April 2024 with an area of low and relatively large phase variations. (Right) Azimuth spectrum sub-band azimuth offsets for the 5 April 2024.

The acquisition being close to the end of the time-series, large phase variations would have a disproportionate effect in the deformation time-series. To avoid this, we used a first estimate of the interferometric phase connected to that date to subtract large scale phase variations. For that, we applied a spatial filter with a radius of approx. 4 km after masking the area of interest and the low coherence areas (Figure 8).

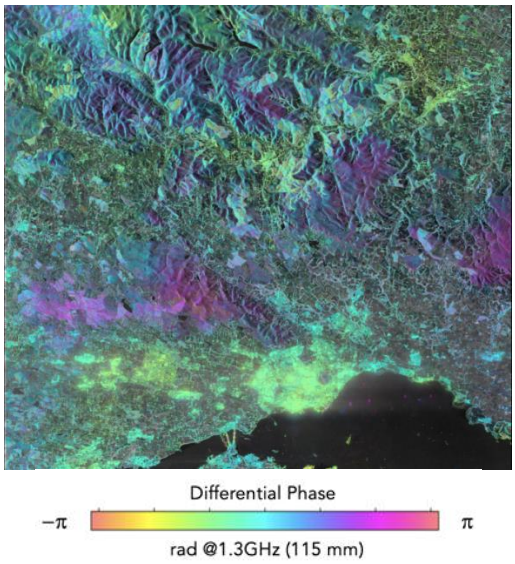

Figure 8. Interferogram of image 5 April 2023 paired with 3 April 2024 after after the refinement of the image substraction of large scale phase variations.

3.4.3 Multi-Looking

To mitigate the effects of low coherence, a multi-looking approach was applied. This technique involves averaging adjacent pixels to reduce noise and improve signal quality. The multi-looking factor used in this case is 3 range looks and 6 azimuth looks.

3.4.4 Phase Unwrapping Iterative Refinement

Phase unwrapping was then performed spatially on strongly multi-looked phase data. This approach helps to smooth out local variations and provides a more stable basis for unwrapping. The phase unwrapping results are then upscaled to the initial sampling and used as a model to re-unwrap the interferograms.

In the following the equivalent single reference time-series was computed as a least squares solution of the multi-reference stack (Werner et al., 2012). A simulated multi-reference stack based on the least squares solution and the standard deviation of the phase residuals were also calculated and used to refine the phase unwrapping of the multi-reference stack, taking advantage of the redundant measurements.

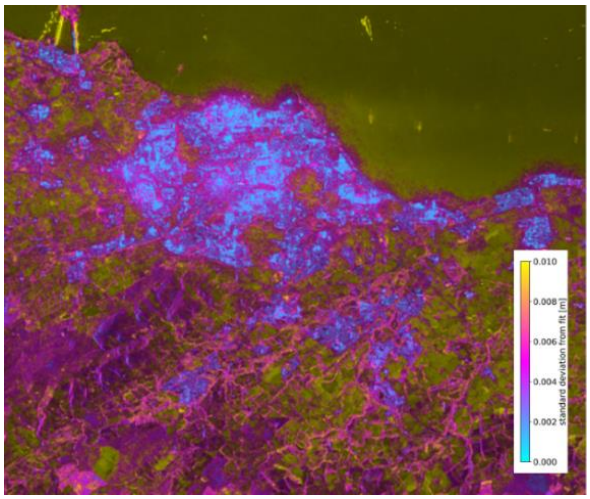

Figure 9. Standard deviation of the phase residuals after the first stage of unwrapping. Yellow shade signify high standard deviation of phase residuals.

The presence of yellow hues in the standard deviation of the phase residuals (Figure 9) typically indicates areas of low coherece and potential phase unwrapping errors. This observation aligns with the geographical context of the study area, which is characterized by dense vegetation cover. Vegetated areas are known to present challenges in interferometric processing due to their temporal

decorrelation and complex scattering properties. The simulated phases of the input interferograms were therefore considered to unwrap separately once again each original interferogram. This process was iteratively performed with each step evaluated for improvement in standard deviation of the phase residuals. After two iterations the standard deviation of the phase residuals has been significantly reduced (Figure 10).

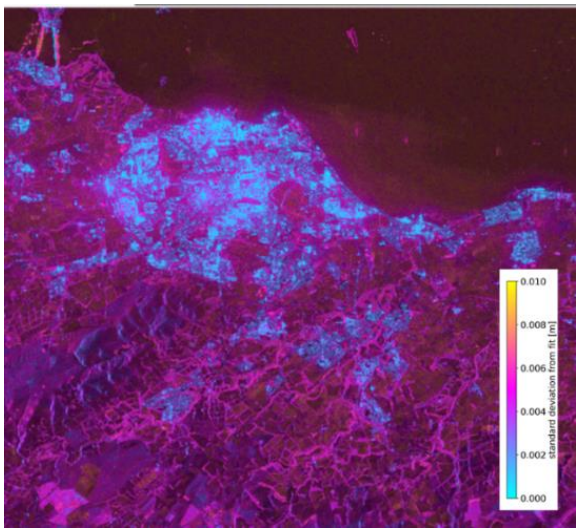

Figure 10. Standard deviation of the phase residuals after two iterations, which has been significantly reduced.

3.5 Time Series Generation

The final phase time-series was calculated by inversion of the set of multi-reference continuous interferograms after two iterations (Werner et al., 2012). In the following, an attempt is made to distinguish between atmosphere and deformation. The process typically involves:

1. alculating the equivalent single reference time-series with and without temporal smoothing.
2. Subtracting the temporally smoothed phase from the unsmoothed phase to retrieve temporally uncorrelated residuals.
3. Estimate a height dependent component of the atmospheric phase based on these residuals
4. Spatially filter the residuals after subtraction of the height dependent component to get an estimate of the turbulent atmospheric phase. We used a filter radius of ~500 m
5. Subtract the estimated atmospheric phase components from the differential phase.

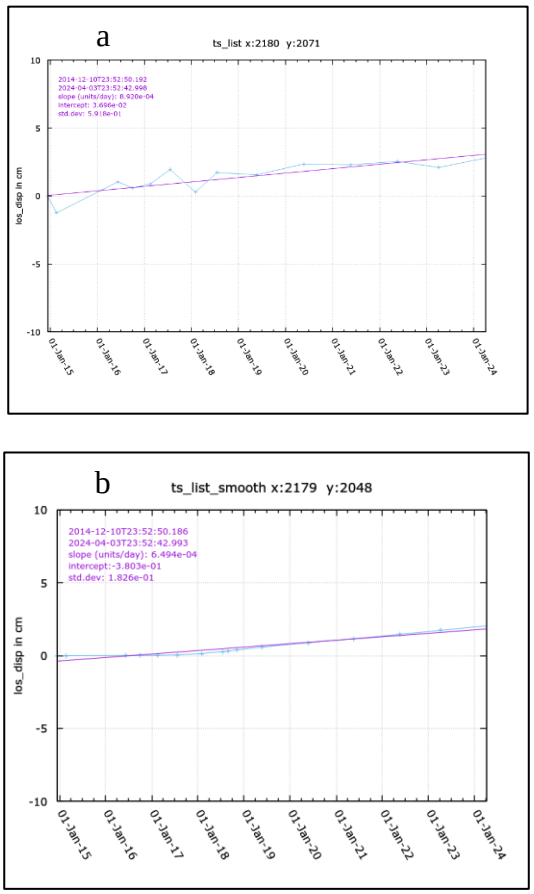

Figure 11. Displacement time series of a point without (a) and (b) with temporal smoothing. For position see red point in the displacement map (c).

These corrections significantly improve the accuracy of displacement measurements, especially in areas with complex topography or variable weather conditions. To further refine the results, a slight temporal filtering was applied, as well as a spatial filtering using an adaptive filter. These steps focus on improving the temporal and spatial coherence of the displacement signal. The process includes identifying and removing outliers or

problematic points in the spatial domain, enhancing the temporal and spatial continuity of the displacement field, and improving the overall visual quality and interpretability of displacement maps.

Spatial filtering helps to reveal more coherent deformation patterns and reduces the impact of localized noise or processing artifacts.

The final step in the time series analysis is the calculation of displacement rates. This process involves conversion of the differential phase values to displacement values, Fitting a linear model to the smoothed and corrected time series data in order to estimate mean deformation rates, and calculation statistical measures of uncertainty for the estimated rates. By following this detailed workflow, the time series analysis produces robust, reliable results that can be confidently used for various applications in geoscience, engineering, and hazard assessment.

4 Results

The time series analysis revealed important insights into the deformation patterns of the area of interest, with notable differences observed between the unsmoothed and smoothed results.

In the unsmoothed version, the results showed a higher variability and noise. Potentially the influences were from atmospheric interference, seasonal effects, temperature fluctuations, vegetation, and soil moisture content changes. The smoothed results offer a more refined view of the long-term deformation patterns, filtering out short-term noise and potential error sources.

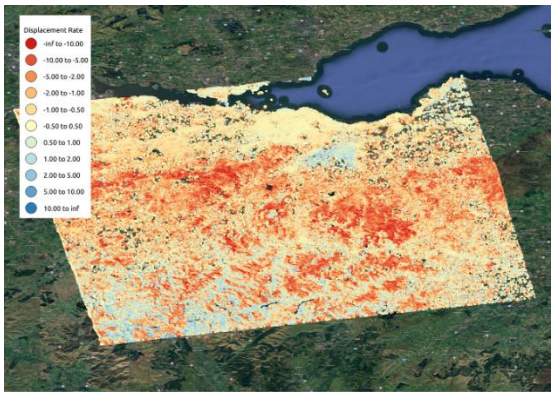

Figure 13. Displacement map with points left and corrected after the spatial and temporal filtering and smoothing.

A closer look to the area of interest is useful to determine and analyze the behavior of the deformation. In this case, we focused on the smoothed version of the result.

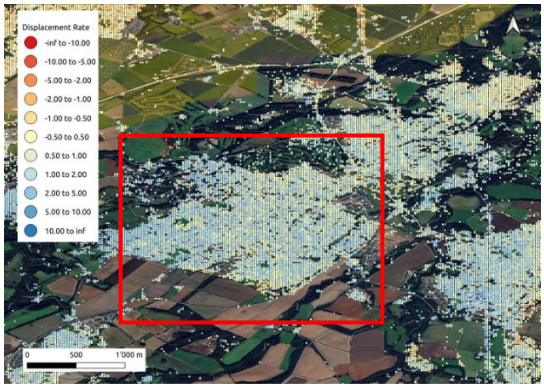

Figure 14. Displacement map with points within the area of Roslyn-Loanhead, the proposed area of the Geobattery project.

To obtain a representative overview of the deformation in the area of interest, around 1000+ points were randomly selected for analysis. This sampling approach provides a statistically significant representation of the overall deformation trend and helps mitigate the impact of potential outliers or localized anomalies.

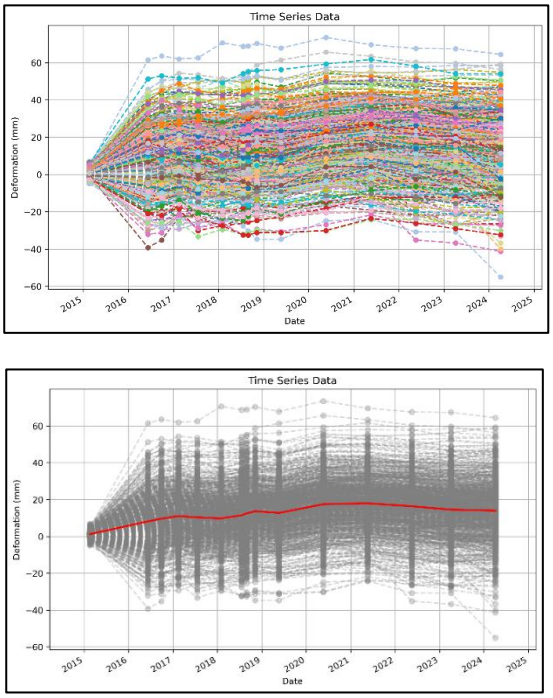

Figure 15. The generated time series of approximately 1000+ points within the area and the aggregate mean of the deformation.

The analysis revealed an average deformation rate of approximately 2-3 mm/year in the area of interest, indicating a slow but consistent ground

movement. This uplift might be noteworthy for the planned Geobattery project in the region as it may affect the socio-economic and other aspects surrounding the area.

5 Conclusion

The resulting displacement rate map provides a comprehensive view of long-term deformation trends across the study area. This information is invaluable for identifying areas of significant ground movement, assessing potential geohazards (e.g., landslides, subsidence, uplift), monitoring infrastructure stability, and supporting decision-making in urban planning and risk management.

Multiple iterations of data filtering and masking was necessary to achieve a satisfactory unwrapped phase and counter the atmospheric interference. Seasonal variations, temperature fluctuations, vegetation, and soil moisture play a significant role in influencing the deformation results. Additionally, the presence of ionospheric artifacts introduces a delay in the radar signal, particularly towards the end of the time series. Despite these challenges, the PSI technique demonstrates significant potential for application in this project.

L-band wavelength tends to be more sensitive to ionospheric condition due to their frequency but provides coherence in heavily vegetated area, resulting in higher coverage compared to other bands. However, at this stage of our research we cannot rule out that systematic bias as reported for Sentinel-1 (Ansari et al., 2021; Maghsoudi et al., 2022) might be also present at L-band.

On the area of Roslyn-Loanhead, our results show some slow uplift deformation. This finding emphasizes the importance of integrating geotechnical and geological assessments into the project planning phase. While the rate is relatively low, it warrants further investigation to determine the underlying causes of the uplift (e.g., geological processes, groundwater changes, or tectonic activity), at the moment, we can assume it's due to the flooding of the mine after the pumping was stopped. A further study on the change of water level will be beneficial. There´s also the need to assess potential long-term impacts on the future project and develop appropriate engineering solutions or adaptations for the project. This involves, integrating multiple sensors (L-band, C-band, and X-band) that cover each other weaknesses and to enhance accuracy of point detection.

Understanding the nature and drivers of this uplift is crucial for ensuring the long-term stability and efficiency of the project, implementing necessary design modifications or mitigation measures, and establishing a robust monitoring program during and after project implementation

References

Edinburgh Geological Society. (2024, December). *Local Geodiversity Sites in Midlothian.* Edinburgh Geological Society. https://www.edinburghgeolsoc.org/home/geoconservation/local-geodiversity-sites-in-midlothian/

Mining Remediation Authority. (2025, February). *Seaham Garden Village*. Mining Remediation Authority https://www2.groundstability.com/seaham/

Ansari, H., De Zan, F., Parizzi, A., 2021. Study of Systematic Bias in Measuring Surface Deformation With SAR Interferometry. IEEE Trans. Geosci. Remote Sens. 59, 1285–1301. https://doi.org/10.1109/TGRS.2020.3003421

Banks, D., Athresh, A., Al-Habaibeh, A., Burnside, N., 2019. Water from abandoned mines as a heat source: practical experiences of open- and closed-loop strategies, United Kingdom. Sustain. Water Resour. Manag. 5, 29–50. https://doi.org/10.1007/s40899-017-0094-7

Banks, D., Fraga Pumar, A., Watson, I., 2009. The operational performance of Scottish minewater-based ground source heat pump systems. Q. J. Eng. Geol. Hydrogeol. 42, 347–357. https://doi.org/10.1144/1470-9236/08-081

Barbier, E., 2002. Geothermal energy technology and current status: an overview. Renew. Sustain. Energy Rev. 6. https://doi.org/10.1016/S1364-0321(02)00002-3

Berardino, P., Fornaro, G., Lanari, R., Sansosti, E., 2002. A new algorithm for surface deformation monitoring based on small baseline differential SAR interferograms. IEEE Trans. Geosci. Remote Sens. 40, 2375–2383. https://doi.org/10.1109/TGRS.2002.803792

Crosetto, M., Monserrat, O., Iglesias, R., Crippa, B., 2010. Persistent Scatterer Interferometry. Photogramm. Eng. Remote Sens. 76, 1061–1069. https://doi.org/10.14358/PERS.76.9.1061

Devanthéry, N., Crosetto, M., Monserrat, O., Cuevas-González, M., Crippa, B., 2014. An Approach to Persistent Scatterer Interferometry. Remote Sens. 6, 6662–6679. https://doi.org/10.3390/rs6076662

Ferretti, A., Prati, C., Rocca, F., 2001. Permanent scatterers in SAR interferometry. IEEE Trans. Geosci. Remote Sens. 39, 8–20. https://doi.org/10.1109/36.898661

Fraser-Harris, A., McDermott, C.I., Receveur, M., Mouli-Castillo, J., Todd, F., Cartwright-Taylor, A., Gunning, A., Parsons, M., 2022. The Geobattery Concept: A Geothermal Circular Heat Network for the Sustainable Development of Near Surface Low Enthalpy Geothermal Energy to Decarbonise Heating. Earth Sci. Syst. Soc. 2, 10047. https://doi.org/10.3389/esss.2022.10047

Gluyas, J.G., Adams, C.A., Wilson, I.A.G., 2020. The theoretical potential for large-scale underground thermal energy storage (UTES) within the UK. Energy Rep. 6, 229–237. https://doi.org/10.1016/j.egyr.2020.12.006

Maghsoudi, Y., Hooper, A.J., Wright, T.J., Lazecky, M., Ansari, H., 2022. Characterizing and correcting phase biases in short-term, multilooked interferograms. Remote Sens. Environ. 275, 113022. https://doi.org/10.1016/j.rse.2022.113022

Meyer, F.J., Nicoll, J., 2008. The Impact of the Ionosphere on Interferometric SAR Processing, in: IGARSS 2008 - 2008 IEEE International Geoscience and Remote Sensing Symposium. Presented at the IGARSS 2008 - 2008 IEEE International Geoscience and Remote Sensing Symposium, IEEE, Boston, MA, USA, p. II-391-II–394. https://doi.org/10.1109/IGARSS.2008.4779010

Nam, B.X., Van Anh, T., Bui, L.K., Long, N.Q., Le Thu Ha, T., Goyal, R., 2021. Mining-Induced Land Subsidence Detection by Persistent Scatterer InSAR and Sentinel-1: Application to Phugiao Quarries, Vietnam, in: Tien Bui, D., Tran, H.T., Bui, X.-N. (Eds.), Proceedings of the International Conference on Innovations for Sustainable and Responsible Mining, Lecture Notes in Civil Engineering. Springer International Publishing, Cham, pp. 18–38. https://doi.org/10.1007/978-3-030-60269-7_2

Strozzi, T., Caduff, R., Jones, N., Manconi, A., Wegmuller, U., 2022. L-Band StripMap-ScanSAR Persistent Scatterer Interferometry in Alpine Environments with ALOS-2 PALSAR-2, in: IGARSS 2022 - 2022 IEEE International Geoscience and Remote Sensing Symposium. Presented at the IGARSS 2022 - 2022 IEEE International Geoscience and Remote Sensing Symposium, IEEE, Kuala Lumpur, Malaysia, pp. 1644–1647. https://doi.org/10.1109/IGARSS46834.2022.9884743

Tulloch, W., Walton, H.S., 1958. The Geology of the Midlothian Coalfield, Memoirs of the Geological Survey ; Economic Memoir, Scotland, Sheet 32, New Series. H.M. Stationery Office.

Van Anh, T., Bui, X.-N., Quoc Long, N., Trung Anh, T., 2020. Land Subsidence Detection in Tan My-Thuong Tan Open Pit Mine and Surrounding Areas by Time Series of Sentinel-1 Images. Inż. Miner. 1. https://doi.org/10.29227/IM-2020-02-22

Wegmuller, U., 1999. Automated terrain corrected SAR geocoding, in: IEEE 1999 International Geoscience and Remote Sensing Symposium. IGARSS'99 (Cat. No.99CH36293). Presented at the IEEE 1999 International Geoscience and Remote Sensing Symposium. IGARSS'99, IEEE, Hamburg, Germany, pp. 1712–1714. https://doi.org/10.1109/IGARSS.1999.772070

Wegmüller, U., Werner, C., Frey, O., Magnard, C., 2024. Estimation and Compensation of the Ionospheric Path Delay Phase in PALSAR-3 and NISAR-L Interferograms. Atmosphere 15, 632. https://doi.org/10.3390/atmos15060632

Wegmüller, U., Werner, C., Strozzi, T., Wiesmann, A., 2002. AUTOMATED AND PRECISE IMAGE REGISTRATION PROCEDURES, in: Analysis of Multi-Temporal Remote Sensing Images. Presented at the Proceedings of the First International Workshop on Multitemp 2001, WORLD SCIENTIFIC, University of Trento, Italy, pp. 37–49. https://doi.org/10.1142/9789812777249_0002

Werner, C., Strozzi, T., Wegmuller, U., 2012. Deformation Time-Series of the Lost-Hills Oil Field using a Multi-Baseline Interferometric SAR Inversion Algorithm with Finite-Difference Smoothing Constraints.

Werner, C., Strozzi, T., Wegmuller, U., Wiesmann, A., 2002. SAR geocoding and multi-sensor image registration, in: IEEE International Geoscience and Remote Sensing Symposium. Presented at the IEEE International Geoscience and Remote Sensing Symposium. IGARSS 2002, IEEE, Toronto, Ont., Canada, pp. 902–904. https://doi.org/10.1109/IGARSS.2002.1025723

Werner, C., Wegmuller, U., Strozzi, T., Wiesmann, A., 2003. Interferometric point target analysis for deformation mapping, in: IGARSS 2003. 2003 IEEE International Geoscience and Remote Sensing Symposium. Proceedings (IEEE Cat. No.03CH37477). Presented at the IGARSS 2003. 2003 IEEE International Geoscience and Remote Sensing Symposium., IEEE, Toulouse, France, pp. 4362–4364. https://doi.org/10.1109/IGARSS.2003.1295516